

# Initial conceptual demonstration of control co-design for WEC optimization

Ryan G. Coe · Giorgio Bacelli · Sterling Olson · Vincent S. Neary ·  
Mathew B. R. Topper

the date of receipt and acceptance should be inserted later

**Abstract** While some engineering fields have benefited from systematic design optimization studies, wave energy converters have yet to successfully incorporate such analyses into practical engineering workflows. The current iterative approach to wave energy converter design leads to suboptimal solutions. This short paper presents an open-source MATLAB toolbox for performing design optimization studies on wave energy converters where power take-off behavior and realistic constraints can be easily included. This tool incorporates an adaptable control co-design approach, in that a constrained optimal controller is used to simulate device dynamics and populate an arbitrary objective function of the user's choosing. A brief explanation of the tool's structure and underlying theory is presented. In order to demonstrate the capabilities of the tool, verify its functionality, and begin to explore some basic wave energy converter design relationships, three conceptual case studies are presented. In particular, the importance of considering (and constraining) the magnitudes of device motion and forces in design optimization is shown.

**Keywords** wave energy converter (WEC) · design optimization · control

R.G. Coe · G. Bacelli · S. Olson · V.S. Neary  
Sandia National Labs, Albuquerque, NM, USA  
Tel.: +1-505-845-9064  
Fax: +1-505-844-6541  
E-mail: rcoe@sandia.gov

M.B.R. Topper  
Data Only Greater, Maynooth, Ireland

## 1 Introduction

At present, designs for wave energy converters (WECs) span a wide range of concepts. While it is unclear which of these concepts will achieve economic viability, the design trade-offs particular to each concept are also not well-defined. Furthermore, the degree to which any of these concepts approach some optimal is also unclear.

Design optimization studies can play an important role in the refinement and maturation of technology concepts. Additionally, a so-called control co-design (CCD) approach, which integrates control system design into full system design process, has been demonstrated for a range of mechanical and electro-mechanical systems (Garcia-Sanz 2019), including a recent study that applied CCD in a full-system constrained design optimization of an offshore wind turbine (Hegseth et al 2020). CCD is composed of three main areas: co-optimization, co-simulation and control-inspired paradigms. In this paper, only the co-optimization aspect is considered, where a lower fidelity multi-physics model is used to carry out a system wide optimization, including the control system.

For resonant WECs in particular, which exhibit tightly-coupled dynamics between the controller and device, a CCD approach appears to be especially useful, perhaps even critical (O'Sullivan and Lightbody 2017; Jin et al 2019). In a system with tightly-coupled dynamics, the dynamics of various subsystem (e.g., the WEC

controller and hydro-mechanical systems) are of overlapping frequency bands. Conversely, in a wind turbine the blade pitch controller acts to reflect changes in wind conditions, which happen on much longer time-scales (over the course of minutes) than blade rotational and tower passing rates, which are on the order of roughly 0.5 Hz.

WEC developers and designers currently lack a systematic, configurable, and tested design optimization tool. As a result, many WEC designs are based on an iterative design-build-test (or often design-model-simulate) loop, which is inefficient and can lead to sub-optimal designs. While a fair amount of WEC design optimization studies have been conducted over the last decade (see, e.g., Blanco et al 2018; Kurniawan and Moan 2013; McCabe 2013), several key limitations have restricted the impact of these studies on practical WEC design. WEC design optimization studies to-date have primarily relied on models that are unable to explicitly incorporate dynamic and kinematic constraints. Additionally, the models employed are unable to incorporate nonlinearities or can only do so at the cost of impractically long computation times.

The present study uses an open-source WEC design optimization tool. The key contributions and fundamental aspects of this tool are:

- **Explicitly model constraints** - Dynamic and kinematic constraints, such as maximum stroke length and maximum power take-off (PTO) force, are critical to ensuring realistic design solutions (Garcia-Rosa et al 2015). Instead of deeming solutions that exceed constraints as infeasible and disregarding them (see, e.g., McCabe 2013), the pseudo-spectral model applied in the present study allows for explicit incorporation of constraints.
- **Efficiently model nonlinear dynamics** - Most previous WEC design optimization studies have employed frequency domain models, which are incapable of handling nonlinearities. Conversely, it is possible for studies to be executed with time domain models (Garcia-Teruel et al 2019), but this approach is computationally expensive. The pseudo-

spectral models employed in this study are capable of efficiently handling nonlinearities. In general, any nature of nonlinearity can be included by representing the physics in the pseudo-spectral domain.

- **Arbitrary or fixed structure controller** - No fixed controller structure (e.g., proportional damping feedback resonating control, latching, or velocity tracking model predictive control) specification is required. The optimal controller can be calculated as the solution to the numerical optimal control problem, or the optimal tuning of a fixed structure control.
- **Open-source tool** - An open-source piece of software, named “WecOptTool,” which is available online,<sup>1</sup> has been developed to perform this study and support future work.

The subsequent sections of this paper are structured to further expand on these points. First the theoretical basis and algorithmic structure are discussed (Section 2). Next, three simple case studies are performed to demonstrate and verify WecOptTool’s functionality in the areas of WEC geometry and PTO co-design and explore some basic design considerations (Section 3). In particular, these case studies have been selected to both illustrate the key aspects of WecOptTool and to begin an exploration of the WEC control co-design space. Conclusions are presented in Section 4.

## 2 Methods

### 2.1 WecOptTool Conceptual Framework

WecOptTool provides WEC developers with a framework to easily apply a control co-design approach. In Fig. 1, the algorithmic procedure is visually classified into three columns or lanes:

- **User Inputs** (Green) - aspects of the tool that the user can interact with
- **Data Classes** (Blue) - objects used to store and transfer information within a study

<sup>1</sup> <https://github.com/SNL-WaterPower/WecOptTool>.

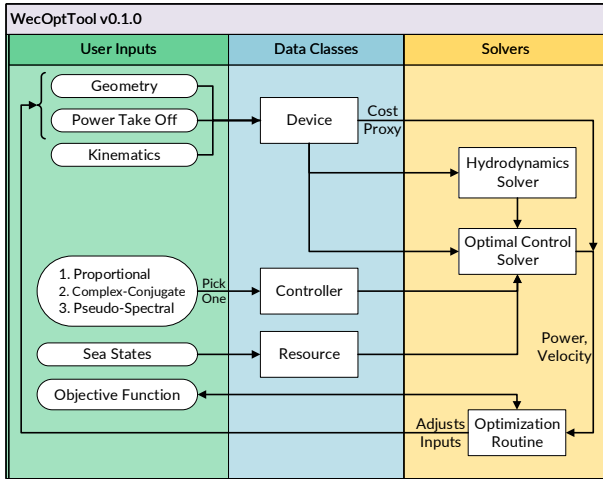


Fig. 1: WecOptTool schematic of data flow to determine an optimal control co-design. The flow from left to right defines the necessary user inputs, how those inputs are mapped to the solvers to determine an optimal design.

156 offered methods (proportional, complex-conjugate, and  
 157 pseudo-spectral – the theoretical basis of these approaches  
 158 is discussed in Section 2.2) to find the WEC velocity,  
 159 PTO forces, power and other dynamic responses of the  
 160 current WEC design. These responses, along with mea-  
 161 sures of cost, can be passed to the objective function for  
 162 use by the optimization routine. By design, WecOpt-  
 163 Tool is meant to leverage existing optimization algo-  
 164 rithms and tools, such as those built into MATLAB  
 165 and other third party tools.

## 166 2.2 Control design and simulation

167 To evaluate device performance, WecOptTool relies pri-  
 168 marily on a pseudo-spectral (PS) solution method (see,  
 169 e.g., Elnagar et al 1995). This numerical optimal con-  
 170 trol method allows for the efficient simulation of non-  
 171 linear dynamics and constrained optimal control of a  
 172 WEC (Bacelli and Ringwood 2014; Bacelli 2014; Herber  
 173 and Allison 2013). The importance of this approach can  
 174 be understood by considering the bounds of the WEC  
 175 control problem.

176 The upper bound of power absorption for a WEC  
 177 is represented by the well-known “complex conjugate  
 178 control,” (CC) in which perfect impedance matching  
 179 allows for maximum power absorption (see, e.g., Falnes  
 180 2002). The intrinsic impedance of a WEC is defined as:

$$181 Z_i(\omega) = B(\omega) + b_v + i \left( \omega(m + A(\omega)) - \frac{K_{HS}}{\omega} \right), \quad (1)$$

182 where  $\omega$  is the radial frequency,  $B(\omega)$  is the radiation  
 183 damping,  $b_v$  accounts for viscous and frictional damp-  
 184 ing,  $m$  is the rigid body mass,  $A(\omega)$  is the added mass,  
 185 and  $K_{HS}$  is the hydrostatic stiffness. The response of  
 186 the device can thus be defined by

$$187 V(\omega) = \frac{F_{exc}(\omega) - F_u(\omega)}{Z_i(\omega)}, \quad (2)$$

188 where  $F_{exc}$  is the wave excitation spectrum.

189 Optimal power transfer occurs when the PTO force,  
 190  $F_u$  is set such that

$$191 F_u(\omega) = -Z_i^*(\omega) u(\omega). \quad (3)$$

131 – **Solvers** (Yellow) - physics models and optimization  
 132 algorithms that process data

133 Any WEC can be optimized by specifying the blocks  
 134 in the User Inputs lane. Consider, for example, the fa-  
 135 mous Salter Duck (Salter 1974). First, the kinematics  
 136 of this device must be defined; for the Salter Duck this  
 137 is a pitching rotation about an axis. Next, the aspects  
 138 of the Duck to be optimized must be chosen, and some  
 139 bounds provided for their values. These design variables  
 140 could include geometric parameters, such as the length  
 141 of the Duck’s “bill,” as well as aspects of the PTO sys-  
 142 tem, such as maximum force, or generator winding re-  
 143 sistance. The wave climate in which the device will op-  
 144 erate (i.e., the sea states in Fig. 1) must be described.  
 145 Additionally, the type of controller to be used should be  
 146 selected (more details on these options in Section 2.2).  
 147 Finally, an objective function is defined to provide a  
 148 measure of fitness based on performance and cost.

149 These user inputs are employed to construct a set  
 150 of Data Class objects (see blue center lane in Fig. 1),  
 151 which are then passed to a set of Solvers (yellow right-  
 152 most lane). The hydrodynamics solver currently used in  
 153 WecOptTool is the boundary element method (BEM)  
 154 tool NEMOH (Babarit and Delhommeau 2015). Cur-  
 155 rently, the optimal control solver uses one of the three

192 where  $Z_i^*$  denotes the complex conjugate of  $Z_i$  and  $u$   
 193 is the velocity. In addition to being acausal in the gen-  
 194 eral sense, this approach specified by (3) is also im-  
 195 practical due to the large motions and forces that often  
 196 result. While analysis of this limit can provide some  
 197 useful insight, it is also clear to see that using an un-  
 198 constrained optimal controller could result in unrealis-  
 199 tic performance (Budal and Falnes 1975), and therefore  
 200 unrealistic values for an objective function within a de-  
 201 sign optimization study.

202 Proportional damping (P) control, which is analo-  
 203 gous to that applied in other energy generation fields in  
 204 which a simple braking force is applied to the generator,  
 205 is a proportional control on velocity:

$$206 F_u = -B_{pto} V, \quad (4)$$

207 where the PTO damping coefficient  $B_{pto}$  is calculated  
 208 by an unconstrained numerical optimization for a given  
 209 sea state.

210 We can see that (2) is a linear frequency domain  
 211 model. Thus, when simulated in this manner, the P  
 212 and CC controllers cannot readily incorporate nonlin-  
 213 earities. Solving for the WEC response in the time do-  
 214 main for an optimization tool is computationally pro-  
 215 hibitive. Fortunately, as described more fully by Ba-  
 216 celli (2014), nonlinearities can be incorporated into a  
 217 pseudo-spectral problem without increasing computa-  
 218 tional time to unmanageable levels. For example, in-  
 219 stead of a linear viscous damping product  $F_v(\omega) =$   
 220  $B_v(\omega) \cdot V(\omega)$ , as applied in (1), viscous damping ef-  
 221 fects can be described by a quadratic term, e.g.,  $F_v =$   
 222  $B_{v2} V|V|$ .

223 The PS controller in WecOptTool has been config-  
 224 ured to maximize power absorption subject to a set of  
 225 constraints. For the PS controller, the dynamics of the  
 226 device are solved by forming an optimization problem in  
 227 which the dynamics are represented as constraints and  
 228 the objective function is formulated to maximize power.  
 229 The system states (in this case WEC position and ve-  
 230 locity) and control inputs are composed by a set of basis  
 231 functions – in this case we use Fourier series. A solution  
 232 is obtained by setting the weights for the basis functions  
 233 so as to minimize the objective function within the con-

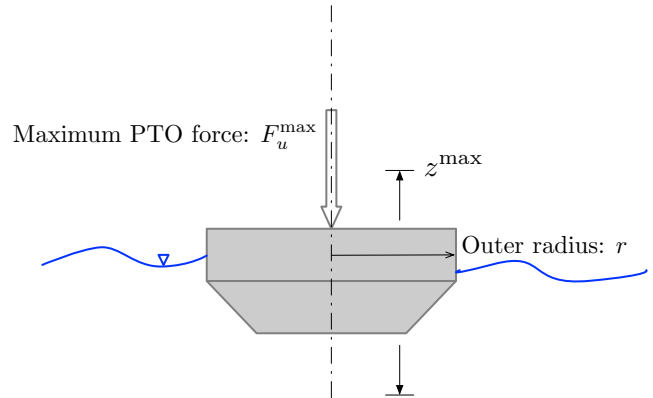


Fig. 2: WaveBot case study design variables.

234 straints (Elnagar et al 1995; Herber and Allison 2013)  
 235 Additionally, realistic constraints, such as limitations  
 236 on the PTO force or stroke length, can be imposed (Ba-  
 237 celli and Ringwood 2014; Bacelli 2014). Currently, We-  
 238 cOptTool applies a sequential quadratic programming  
 239 (SQP) solution method ( Nocedal and Wright 2006) for  
 240 the pseudo-spectral problem. For the CCD problem,  
 241 this approach offers a number of distinct advantages to  
 242 frequency domain and time-domain models as described  
 243 in Section 1 (explicit constraints, efficient nonlinear so-  
 244 lutions, and arbitrary or fixed controller structures).

245 Currently, the PS controller in WecOptTool uses an  
 246 arbitrary control structure. Thus, while the WEC may  
 247 eventually be deployed with a causal feedback controller  
 248 (Bacelli and Coe 2020; Bacelli et al 2019; Scruggs et al  
 249 2013), a latching controller (Budal and Falnes 1979;  
 250 Evans 1976; Iversen 1982), or a velocity tracking model  
 251 predictive control (Cretel et al 2011; Hals et al 2011),  
 252 the arbitrary PS controller in WecOptTool provides a  
 253 convenient *realistic stand-in* for design studies. The PS  
 254 controller in WecOptTool is not intended for real-time  
 255 implementation, but instead represents a control design  
 256 and analysis tool.

### 257 3 Case studies

258 The design of the experimental “WaveBot” (Coe et al  
 259 2016) is considered herein to provide a case study on  
 260 which to apply WecOptTool and demonstrate impor-  
 261 tant concepts in WEC co-control design. Fig. 2 shows

Table 1: Summary of case study parameters. See Fig. 2, for illustration of variables.

Design variable	Case A	Case B	Case C
Outer radius, $r$ [m]	$r = 0.88$	$r \in [0.25, 2]$	$r \in [0.25, 2]$
Maximum PTO force, $F_u^{\max}$ [kN]	$F_u^{\max} = 2$	$F_u^{\max} = \infty$	$F_u^{\max} \in [0.1, 1]$
Maximum stroke, $z^{\max}$ [m]	$z^{\max} = \infty$	$z^{\max} = 0.6$	$z^{\max} = \infty$

an illustration of the device and the design variables employed in these case studies. Three different case studies of the WaveBot are considered: (A) a simple fixed design performance assessment demonstrating and verifying the CC, P, PS controllers, (B) a single design variable study comparing the CC, P, and PS controllers, and (C) a multi-objective study using only the PS controller. For efficiency and to improve clarity, all studies were conducted using a simple regular wave with an amplitude of  $A = 0.0625$  m and a period of  $T = 3.33$  s. These case studies are summarized in Table 1.

It is important to note the case studies in this paper are conceptual in nature. While more complex and realistic studies are possible with WecOptTool, these case studies have been deliberately selected to verify functionality and to demonstrate key concepts in WEC CCD. Although simplistic, these case studies describe phenomena and approaches that are fundamental to the engineering practice of WEC control co-design. A strong understanding of these concepts is essential for future applications of WecOptTool to more complex studies.

### 3.1 Case A: Performance with CC, P, and PS controllers

Case A is not a design optimization study, but instead a simple comparison of the three controller types' performance using a single device design. Thus, the device design was fixed, and the performance in a regular wave with  $A = 0.0625$  m,  $T = 3.33$  s was simulated for the CC, P, and PS controllers. The PS controller was set to limit the PTO force to less than 2 kN. The results of these simulations are shown in Fig. 3 and Fig. 4, which show the spectral and time-history results, respectively. The average mechanical powers for the three controllers

in Case A were CC: 121 W; P: 28 W; and PS: 97 W. Note that as the PTO force limit for the PS controller is increased, the power from this controller will approach that of the CC controller.

Fig. 3 shows a spectral analysis of results from the Case A simulations, with magnitude along the upper row and phase along the lower row. Each of the three columns of plots relate to a specific controller. The spectra of excitation force ( $F_e$ ), velocity ( $u$ ), and PTO force ( $F_u$ ) resulting from each simulation are plotted. We can verify the linear behavior of the CC and P controllers by reviewing the left and center columns in Fig. 3, respectively. The linear behavior of these controllers is evident in that energy exists only at the excited frequency of 1.89 rad/s ( $T = 3.33$  s). Also note how the CC controller creates a resonant condition, where the velocity has the same phase as the excitation force, whereas the P controller does not achieve this phase alignment. From the results of the PS controller on the far right of Fig. 3, it can be seen that the velocity at 1.89 rad/s is nearly in phase with the excitation force. The slight mismatch is due to the PTO force limit.

Observe how super-harmonics are generated by the force limited PS controller, spilling energy into additional frequencies, which are integer multiples of the fundamental. These additional harmonics outside of the fundamental excited frequency ( $1\omega_0 = 1.89$  rad/s) are a clear demonstration of the nonlinearities introduced by the PS controller. In order to maximize power while limiting the PTO force ( $|F_u| < 2$  kN), the PS controller finds this nonlinear solution.<sup>2</sup>

<sup>2</sup> Note that, as discussed in Section 2.2, it would also be possible to include additional nonlinearities within the WEC dynamics for the PS controller (e.g., nonlinear damping due fluid viscosity and/or friction, switching in the PTO, etc.). In this example, we have chosen not to include such effects so as to provide a more direct comparison with the C and P controllers, which have been programmed in the frequency

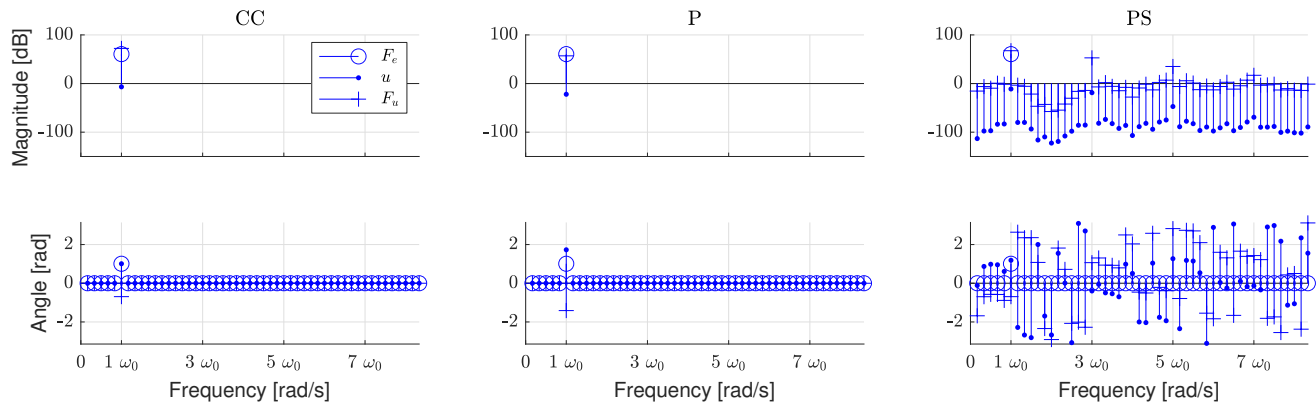


Fig. 3: Case A: Spectral analysis of CC, P, and PS simulation results for a single device design.

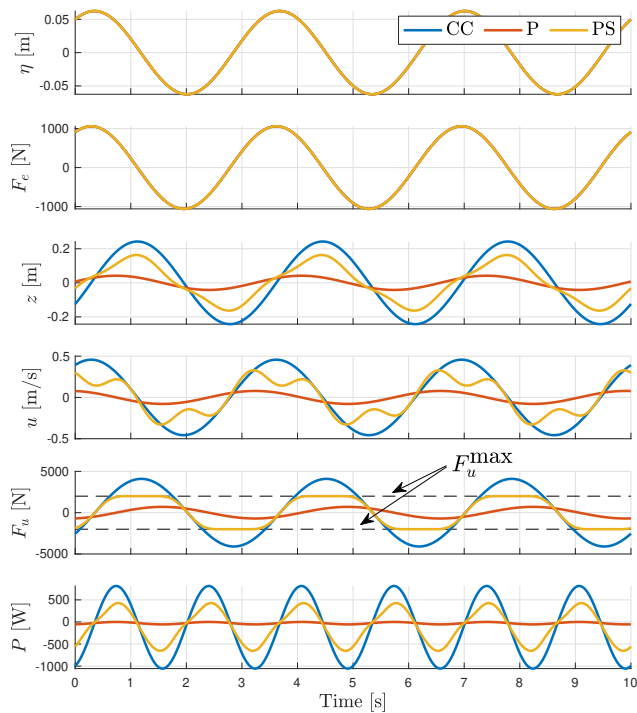


Fig. 4: Case A: Comparison of time histories of CC, P, and PS controllers for a single device design.

335 magnitude of instantaneous power created by the CC  
336 controller, both negative (resistive) and positive (reac-  
337 tive), is also evident.

### 338 3.2 Case B: Optimal design for CC, P, and PS 339 controllers

340 The differences between these controllers and the im-  
341 portance of control co-design can further be demon-  
342 strated by considering how the optimal device design  
343 varies with different control strategies. To better un-  
344 derstand this we conduct three separate optimization  
345 studies using the CC, P, and PS controllers. These stud-  
346 ies are performed on the following problem.

$$\begin{aligned}
 & \min_r \frac{\bar{P}(r)}{(r_0 + r)^3} \\
 & \text{s.t. } r \in [0.25, 2]
 \end{aligned} \tag{5}$$

348 Here,  $r$  is the WEC's outer radius as shown in Fig. 2.  
349 The radius of the WaveBot as-built (that tested by Coe  
350 et al 2016) is  $r_0 = 0.88$  m. The average power is  $\bar{P}$ ,  
351 where negative power is absorbed by the device. The  
352 maximum stroke of the PS controller was constrained  
353 to  $z^{\max} \leq 0.6$  m.

354 At this stage, the specification of an objective func-  
355 tion for WEC design optimization is quite challenging  
356 given the diverse spectrum of WEC archetypes and the  
357 lack of commercial projects. The objective function de-  
358 fined by (5) is similar to those suggested by a number  
359 of previous studies, in that it is a ratio of power to  
360 some representation of cost – volume in this case, but

327 The time histories of the Case A simulations shown  
328 in Fig. 4 tell a similar story and verify the expected be-  
329 havior of these controllers. The six axes in Fig. 4 from  
330 top to bottom show the wave elevation ( $\eta$ ), excitation  
331 force ( $F_e$ ), position ( $z$ ), velocity ( $u$ ), PTO force ( $F_u$ ),  
332 and power ( $P$ ), where negative power is absorbed by  
333 the WEC. The PS controller follows the CC controller  
334 until it reaches the force limitation of 2 kN. The large  
domain for efficiency and can thus not readily incorporate  
nonlinear dynamics.

Table 2: Case B: Comparison of optimal WaveBot designs for different controllers.

Controller	Opt. radius, $r_{\text{opt}}$	Obj. fun. value
CC	0.25	-86.1
P	1.00	-5.0
PS	0.40	-47.7

surface area has also been recommended (Garcia-Teruel et al 2019; Blanco et al 2018; Kurniawan 2013; McCabe 2013). Garcia-Teruel et al (2019) present a useful comparison where various combinations of these factors are used to form different objective functions, thus leading to different optimal WEC designs. Note that (5) uses a polynomial expansion in the denominator, as was done previously by Neary et al (2018) to counteract the effect where small devices are disproportionately favored.

The study was completed with both a “brute-force” approach and using the MATLAB hybrid method solver `fminbnd`. The set of geometries considered are shown in Fig. 5. Table 2 shows the results of this study for each of the three control types. The results are also illustrated in Fig. 6.

As can be seen from Fig. 6 and Table 2 the results from the three different controllers vary dramatically. The power produced by the CC controller is often an order of magnitude greater than the P controller. Note that, accounting for friction, the power absorbed by the CC controller matches the theoretical limit for an axisymmetric body (Budal and Falnes 1975).

Additionally, the power produced by the CC controller does not vary strongly based on the outer radius design variable. This occurs because the complex-conjugate controller can so effectively maximize absorption that the geometry of the WEC (assuming it is of the same general scale) plays a less important role. This is not necessarily realistic, a problem which can be further illustrated by considering the position amplitudes shown in Fig. 6. The CC controller can only accomplish this feat at low frequencies by moving the WEC with an amplitude of more than 1 m (in a 0.06 m amplitude wave). Obviously this motion violates the assumptions of the underlying models, but would also likely require an unfeasible design. Observe also that for radius val-

ues of  $r > 0.55$  m, the PS and CC results match, but for  $r < 0.55$  m, the motion constraint becomes active for the PS controller.

Referring back to the overall results of the study in Table 2, note that the three controllers result in different optimal designs. While this is not surprising based on the conclusions drawn from Case A (Section 3.1) and the results shown in Fig. 6, and also aligns with previous findings (Garcia-Rosa and Ringwood 2016), this outcome underscores the importance of incorporating realistic physical constraints when applying CCD. A WEC device’s performance, and therefore the objective function value, is strongly tied to the controller, thus it follows that designing the controller in parallel with the full system is critical.

### 3.3 Case C: Multi-objective design study

It is often beneficial for practical WEC design studies to employ a multi-objective optimization. For the WaveBot in particular, which is a lab device with no full-scale deployment plan, and therefore no detailed means of estimating LCOE, such an approach is especially useful. In a multi-objective study, a set of “responses” can be selected without applying any relative weighting factors that may be challenging, or impossible, to determine. In this way, a better understanding for how the design variables interact can be developed.

In this case, we consider the following problem:

$$\begin{aligned}
 & \min_{r, F_u^{\max}} \quad (\bar{P}, (r_0 + r)^3, z^{\max}) \\
 & \text{s.t.} \quad r \in [0.25, 2] \\
 & \quad \quad F_u^{\max} \in [0.1, 1] \times 10^3
 \end{aligned} \tag{6}$$

Here  $\bar{P}$  and  $(r_0 + r)^3$  are the average power and a volumetric function, as were used in Case B. The third response,  $z_{\max}$ , is the maximum displacement position of the WEC (PTO “stroke”). As before, the outer radius,  $r$ , is a design variable with the range  $[0.25, 2]$  m. However, in Case C, the additional design variable for the maximum PTO force,  $F_u^{\max}$ , is added with a range of  $[0.1, 1]$  kN. Note that since it is considered the best suited solution for a CCD optimization study, only the

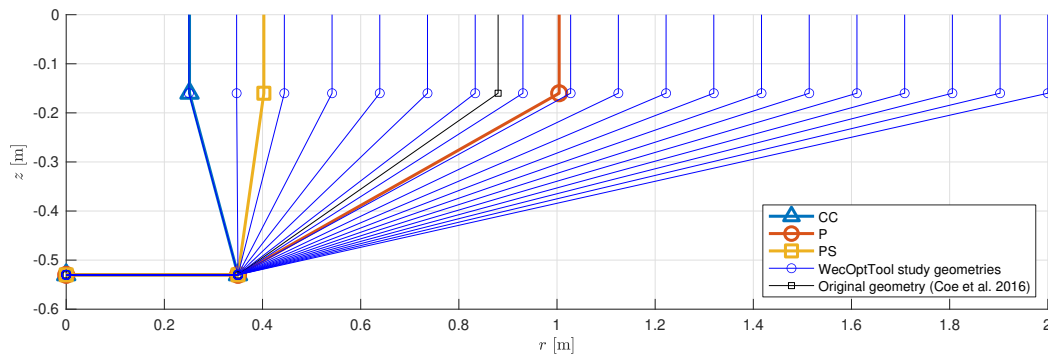


Fig. 5: Case B: WaveBot geometries (shown via axisymmetric cross-section) considered via brute force.

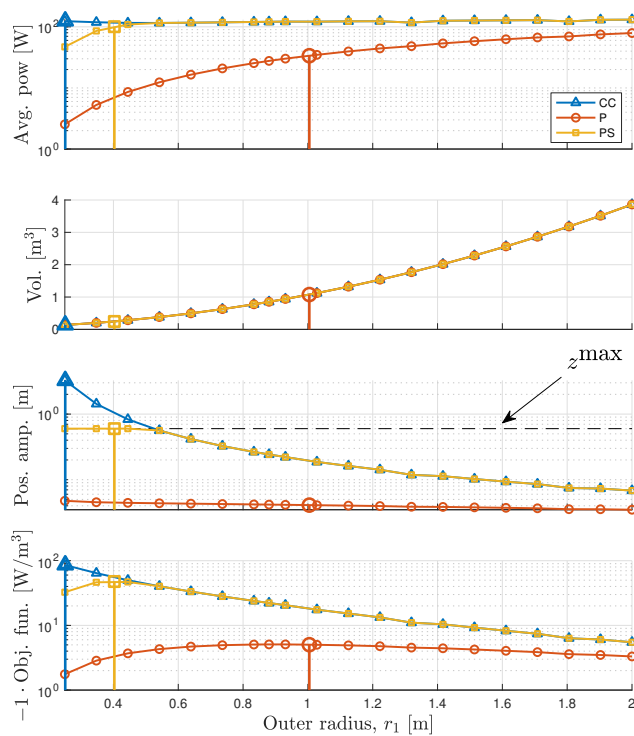


Fig. 6: Case B: study results. Vertical stems show optimal designs from `fminbnd`.

ables and responses interact. Reviewing Fig. 7, we can see that smaller designs require larger PTO strokes to achieve the same amount of power absorption (a similar finding was noted by Kurniawan 2013). Based on this, a designer could weigh the factors that affect cost (longer PTO pistons vs. increasing hull displacement – and the numerous factors tied to these variables, such as structural reinforcement, mooring design, etc.).

To find a single solution along the Pareto front, it is typical to find a “knee” in the curve or surface, in which a marginal improvement of one objective function would lead to large decline in others (see, e.g., Branke et al 2004). One potential knee on the surface shown in Fig. 7 has been marked with a ‘+.’ Here, the WEC produces an average of 58 W, with a volume function of  $(r_0 + r)^3 = 3.9 \text{ m}^3$ , and a maximum PTO stroke of 0.14 m.

#### 4 Conclusion

An open source WEC design optimization tool, that provides an adaptable engineering approach to control co-design, has been demonstrated and verified via three different case studies. These studies highlight the utility of the tool, in particular the important contribution of utilizing a pseudo-spectral numerical optimal control solution that can realistically represent constrained WEC controllers. The inclusion of the pseudo-spectral method allows for efficient and realistic control co-design studies to be performed.

pseudo-spectral control method was used in Case C (as previously discussed, complex-conjugate and proportional damping control are more useful for theoretical studies). This study was performed with the MATLAB function `paretosearch`, which uses a pattern search algorithm.

The results of this case study are shown in Fig. 7. As with any multi-objective study, no single device design is shown to be most fit, but the designer can begin to gain some intuition on how these different design vari-

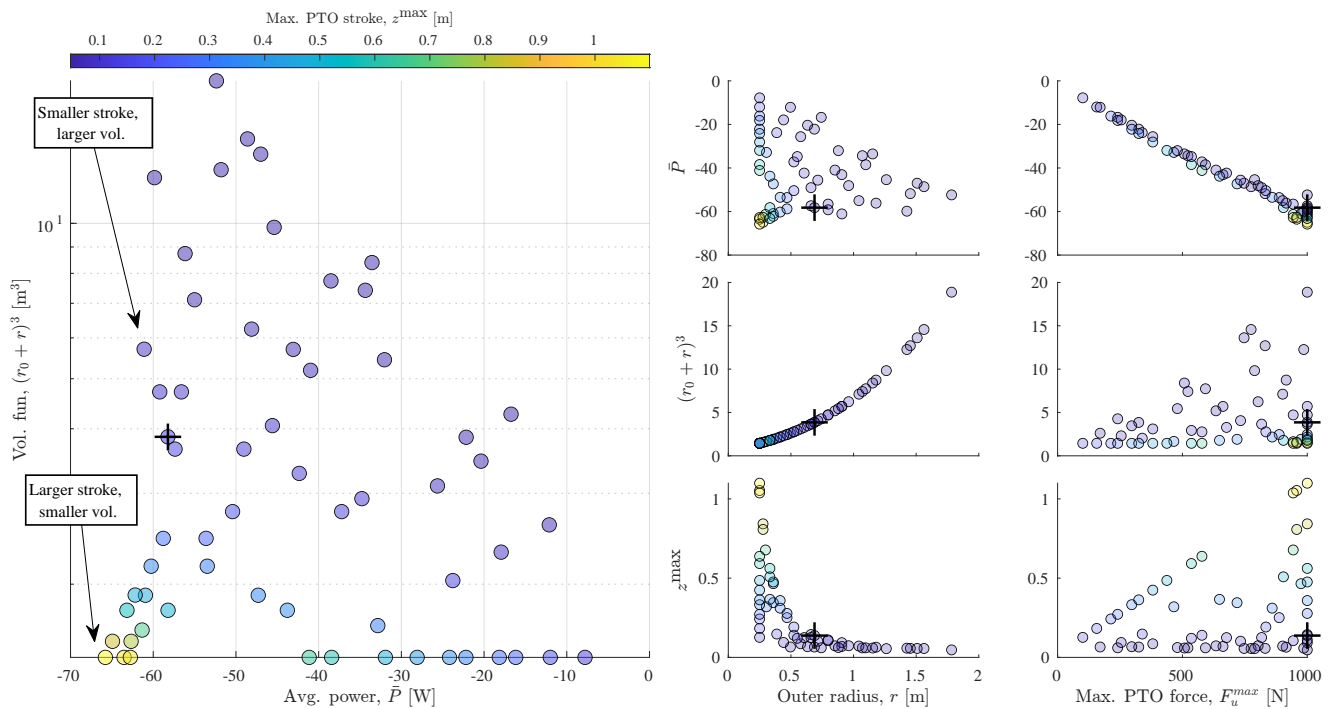


Fig. 7: Case C: multi-objective optimization results. Color of points corresponds maximum PTO stroke,  $z^{\max}$ . Larger plot on left-hand side shows the Pareto front most intuitively; six smaller plots to right-hand side show all projections of results, with each column pertaining to a design variable ( $r$  and  $F_u^{\max}$ ) and each row pertaining to an objective function ( $\bar{P}$ ,  $(r_0 + r)^3$ , and  $z_{\max}$ ). Potential single solution at knee on surface marked with ‘+’.

472 Future development of WecOptTool will introduce  
 473 both linear and nonlinear classes of fixed structure con-  
 474 trollers. Additionally, further recent developments in  
 475 formulations for integrated PTO modeling will be in-  
 476 corporated into WecOptTool to allow for more detailed  
 477 studies. By treating an array of WECs as an abstract  
 478 multi-input, multi-output system, WecOptTool can also  
 479 potentially be applied to WEC array design and used,  
 480 for example, to determine device spacing within the ar-  
 481 ray. To support more straightforward utilization by a  
 482 wider range of users, additional WEC archetypes will  
 483 be examined in case studies and provided as examples  
 484 with the WecOptTool source code. Further case studies  
 485 will also seek to investigate the formulation of objective  
 486 functions for WEC design optimization studies, and to  
 487 perform such studies using realistic WECs with real-  
 488 world deployment locations.

489 **Acknowledgements** Sandia National Laboratories is a multi-  
 490 mission laboratory managed and operated by National Tech-  
 491 nology and Engineering Solutions of Sandia, LLC., a wholly

492 owned subsidiary of Honeywell International, Inc., for the  
 493 U.S. Department of Energy’s National Nuclear Security Ad-  
 494 ministration under contract DE-NA0003525. This paper de-  
 495 scribes objective technical results and analysis. Any objec-  
 496 tive views or opinions that might be expressed in the paper  
 497 do not necessarily represent the views of the U.S. Department  
 498 of Energy or the United States Government.

## 499 References

- 500 Babarit A, Delhommeau G (2015) Theoretical and numer-  
 501 ical aspects of the open source BEM solver NEMOH.  
 502 In: 11th European Wave and Tidal Energy Confer-  
 503 ence (EWTEC2015), Nantes, France, URL [https://hal.  
 504 archives-ouvertes.fr/hal-01198800](https://hal.archives-ouvertes.fr/hal-01198800)  
 505 Bacelli G (2014) Optimal control of wave energy con-  
 506 verters. PhD thesis, National University of Ireland,  
 507 Maynoot, Ireland, URL [https://core.ac.uk/download/  
 508 pdf/297020291.pdf](https://core.ac.uk/download/pdf/297020291.pdf)  
 509 Bacelli G, Coe RG (2020) Comments on control of wave en-  
 510 ergy converters. IEEE Transaction on Control System  
 511 Technologies DOI 10.1109/TCST.2020.2965916, URL  
 512 <https://ieeexplore.ieee.org/document/9005201>  
 513 Bacelli G, Ringwood JV (2014) Numerical optimal con-  
 514 trol of wave energy converters. IEEE Transactions

- 515 on Sustainable Energy 6(2):294–302, DOI 10.1109/  
516 TSTE.2014.2371536, URL <https://ieeexplore.ieee.org/document/6987295>
- 517 Bacelli G, Nevarez V, Coe RG, Wilson D (2019) Feedback  
518 resonating control for a wave energy converter. IEEE In-  
519 dustrial Automation and Control 56(2), DOI 10.1109/  
520 TIA.2019.2958018, URL <https://ieeexplore.ieee.org/abstract/document/8926523>
- 521 Blanco M, Lafoz M, Ramirez D, Navarro G, Torres J, Garcia-  
522 Tabares L (2018) Dimensioning of point absorbers for  
523 wave energy conversion by means of differential evolution-  
524 ary algorithms. IEEE Transactions on Sustainable En-  
525 ergy 10(3):1076–1085, DOI 10.1109/TSTE.2018.2860462,  
526 URL <https://ieeexplore.ieee.org/document/8421039>
- 527 Branke J, Deb K, Dierolf H, Osswald M (2004) Find-  
528 ing knees in multi-objective optimization. In: Par-  
529 allel Problem Solving from Nature - PPSN VIII,  
530 Springer Berlin Heidelberg, Berlin, Heidelberg, pp  
531 722–731, URL [https://link.springer.com/chapter/10.1007/978-3-540-30217-9\\_73](https://link.springer.com/chapter/10.1007/978-3-540-30217-9_73)
- 532 Budal K, Falnes J (1975) A resonant point absorber of  
533 ocean-wave power. Nature 256(5517):478–479, DOI 10.  
534 1038/256478a0, URL <http://www.nature.com/nature/journal/v256/n5517/abs/256478a0.html>
- 535 Budal K, Falnes J (1979) Interacting point absorbers with  
536 controlled motion. In: Count B (ed) Power from Sea  
537 Waves, Academic Press London, Edinburgh, Scotland, pp  
538 381–399
- 539 Coe RG, Bacelli G, Patterson D, Wilson DG (2016) Ad-  
540 vanced WEC Dynamics & Controls FY16 testing re-  
541 port. Tech. Rep. SAND2016-10094, Sandia National  
542 Labs, Albuquerque, NM, URL <https://mhkdr.openei.org/submissions/151>
- 543 Cretel J, Lightbody G, Thomas G, Lewis A (2011) Max-  
544 imisation of energy capture by a wave-energy point ab-  
545 sorber using model predictive control. vol 44, pp 3714 –  
546 3721, DOI <https://doi.org/10.3182/20110828-6-IT-1002.03255>, URL <http://www.sciencedirect.com/science/article/pii/S1474667016441893>, 18th IFAC World  
547 Congress
- 548 Elnagar G, Kazemi M, Razzaghi M (1995) The pseudospec-  
549 tral legendre method for discretizing optimal control  
550 problems. Automatic Control, IEEE Transactions on  
551 40(10):1793–1796, DOI 10.1109/9.467672
- 552 Evans DV (1976) A theory for wave-power absorption  
553 by oscillating bodies. Journal of Fluid Mechan-  
554 ics 77(01):1–25, DOI 10.1017/S0022112076001109,  
555 URL <http://journals.cambridge.org/action/displayAbstract?fromPage=online&aid=374123>
- 556 Falnes J (2002) Ocean Waves and Oscillating Systems. Cam-  
557 bridge University Press, Cambridge; New York
- 558 Garcia-Rosa PB, Ringwood JV (2016) On the sensitivity of  
559 optimal wave energy device geometry to the energy maxi-  
560 mizing control system. IEEE Transactions on Sustainable  
561 Energy 7(1):419–426, DOI 10.1109/TSTE.2015.2423551
- 562 Garcia-Rosa PB, Bacelli G, Ringwood JV (2015) Control-  
563 informed geometric optimization of wave energy con-  
564 verters: The impact of device motion and force con-  
565 straints. Energies 8(12):12386, DOI 10.3390/en81212386,  
566 URL <http://www.mdpi.com/1996-1073/8/12/12386>
- 567 Garcia-Sanz M (2019) Control co-design: an engineering game  
568 changer. Advanced Control for Applications: Engineering  
569 and Industrial Systems 1(1):e18, DOI 10.1002/adc2.18
- 570 Garcia-Teruel A, Forehand D, Jeffrey H (2019) Metrics  
571 for wave energy converter hull geometry optimisation.  
572 In: Proceedings of the 13th Annual European Wave  
573 and Tidal Energy Conference (EWTEC), Naples, Italy,  
574 URL [https://www.researchgate.net/publication/335892704\\_Metrics\\_for\\_Wave\\_Energy\\_Converter\\_Hull\\_Geometry\\_Optimisation](https://www.researchgate.net/publication/335892704_Metrics_for_Wave_Energy_Converter_Hull_Geometry_Optimisation)
- 575 Hals J, Falnes J, Moan T (2011) A comparison of se-  
576 lected strategies for adaptive control of wave energy  
577 converters. Journal of Offshore Mechanics and Arctic En-  
578 gineering 133(3):031101, DOI 10.1115/1.4002735, URL  
579 <http://offshoremechanics.asmedigitalcollection.asme.org/article.aspx?articleid=1456895>
- 580 Hegseth JM, Bachynski EE, Martins JR (2020) Inte-  
581 grated design optimization of spar floating wind  
582 turbines. Marine Structures 72:102771, DOI  
583 10.1016/j.marstruc.2020.102771, URL <https://www.sciencedirect.com/science/article/pii/S0951833920300654>
- 584 Herber DR, Allison JT (2013) Wave Energy Extraction Max-  
585 imization in Irregular Ocean Waves Using Pseudospec-  
586 tral Methods. International Design Engineering Techni-  
587 cal Conferences and Computers and Information in En-  
588 gineering Conference, vol 3A: 39th Design Automation  
589 Conference, DOI 10.1115/DETC2013-12600
- 590 Iversen LC (1982) Numerical method for comput-  
591 ing the power absorbed by a phase-controlled  
592 point absorber. Applied Ocean Research 4(3):173–  
593 180, DOI 10.1016/S0141-1187(82)80054-0, URL  
594 <http://www.sciencedirect.com/science/article/pii/S0141118782800540>
- 595 Jin S, Patton RJ, Guo B (2019) Enhancement of wave  
596 energy absorption efficiency via geometry and power  
597 take-off damping tuning. Energy 169:819 – 832, DOI  
598 <https://doi.org/10.1016/j.energy.2018.12.074>, URL  
599 <http://www.sciencedirect.com/science/article/pii/S036054421832440X>
- 600 Kurniawan A (2013) Modelling and geometry optimisation  
601 of wave energy converters. PhD thesis, Norwegian Uni-  
602 versity of Science and Technology, Trondheim, Norway,  
603 URL <http://hdl.handle.net/11250/238376>
- 604 Kurniawan A, Moan T (2013) Optimal geometries for wave  
605 absorbers oscillating about a fixed axis. IEEE Journal of  
606

- 621 Oceanic Engineering 38(1):117–130, DOI 10.1109/JOE.  
622 2012.2208666
- 623 McCabe A (2013) Constrained optimization of the shape  
624 of a wave energy collector by genetic algorithm. Re-  
625 newable energy 51:274–284, DOI 10.1016/j.renene.2012.  
626 09.054, URL [https://www.sciencedirect.com/science/  
627 article/pii/S0960148112006258](https://www.sciencedirect.com/science/article/pii/S0960148112006258)
- 628 Neary VS, Coe R, Cruz J, Haas K, Bacelli G, Debruyne Y,  
629 Ahn S, Nevarez V (2018) Classification systems for wave  
630 energy resources and WEC technologies. International  
631 Marine Energy Journal 1(2):71–79, DOI 10.36688/imej.  
632 1.71-79, URL <https://doi.org/10.36688/imej.1.71-79>
- 633 Nocedal J, Wright S (2006) Numerical optimization. Springer  
634 Science & Business Media
- 635 O’Sullivan AC, Lightbody G (2017) Co-design of a wave  
636 energy converter using constrained predictive control.  
637 Renewable Energy 102, Part A:142 – 156, DOI  
638 <http://dx.doi.org/10.1016/j.renene.2016.10.034>, URL  
639 [http://www.sciencedirect.com/science/article/pii/  
640 S0960148116308990](http://www.sciencedirect.com/science/article/pii/S0960148116308990)
- 641 Salter SH (1974) Wave power. Nature 249(5459):720–724,  
642 DOI 10.1038/249720a0
- 643 Scruggs JT, Lattanzio SM, Taflanidis AA, Cassidy IL  
644 (2013) Optimal causal control of a wave energy  
645 converter in a random sea. Applied Ocean Re-  
646 search 42:1–15, DOI 10.1016/j.apor.2013.03.004, URL  
647 [http://www.sciencedirect.com/science/article/pii/  
648 S0141118713000205](http://www.sciencedirect.com/science/article/pii/S0141118713000205)